Paper: ASAT-14-032-ST

14th International Conference on
AEROSPACE SCIENCES & AVIATION TECHNOLOGY,
ASAT - 14 – May 24 - 26, 2011, Email: asat@mtc.edu.eg
Military Technical College, Kobry Elkobbah, Cairo, Egypt
Tel: +(202) 24025292 –24036138, Fax: +(202) 22621908

Tension-Bearing Couples (TBC), Part I*: FEM Validation of Proposed Analysis Approach, Approach Enhancement, Results Comparisons and Evaluation

Hatem H. Daken† and M. Kamal Shoukry‡

Abstract: A new approach to analyze fastener joints loaded with out-of-plane forces and moments was introduced in Reference 1. This article discusses the results of eight (8) fastener joints analyzed using the proposed analysis approach as compared to the results of idealized finite element models that were constructed to simulate the properties and behavior of these joints. The fastener joints analyzed entail six (6) low to medium aspect ratio joints and two (2) high aspect ratio joints. Results of the idealized finite element models are within ±10% of the results of the proposed analysis approach.

Keywords: Tension-Bearing Couple, Tensile-Loaded Fasteners, Bolted Joints, Fastener Joints, Finite Element Method, Finite Element Analysis, Finite Element Modeling

1. Nomenclature

b	Width of the fitting
h	Height of the fitting
K_{EF}	Extensional stiffness of the equivalent fastener, which is equal to the total extensional stiffness of all fasteners
K_i	Extensional stiffness of the i^{th} fastener
M	Out-of-plane bending moment vector in the local x-y plane
M_x	Out-of-plane bending moment vector component along the local x-axis
M_y	Out-of-plane bending moment vector component along the local y-axis
P_{MOD}	Predicted value, enhanced analytical model
P_{FEM}	Predicted value, idealized finite element model
$R_{EF, Mx}$	Reaction in the equivalent fastener due to the x-axis component of applied out-of-plane bending moment, M_x
$R_{EF, My}$	Reaction in the equivalent fastener due to the y-axis component of applied out-of-plane bending moment, M_y
t	Thickness of the fitting
$X_{angcorr}$	Adjacent side of the estimated angle between the neutral line and the local x-axis, α_e
X_{FSCG}	X-coordinate of the location of the fasteners stiffnesses centroid
$Y_{angcorr}$	Opposite side of the estimated angle between the neutral line and the local x-axis, α_e
Y_{FSCG}	Y-coordinate of the location of the fasteners stiffnesses centroid

* Refer to the other two parts in this volume

† Ph.D., Senior Structural Analysis Scientist/Engineer, Boeing Commercial Airplanes, The Boeing Company, Seattle, WA, USA, hatemdaken@aol.com

‡ Ph.D., Professor of Design and Production Engineering, German University, Cairo, Egypt

$Z_{EF, Mx}$	Z-axis extension of the equivalent fastener due to the x-axis component of applied out-of-plane bending moment, M_x
$Z_{EF, My}$	Z-axis extension of the equivalent fastener due to the y-axis component of applied out-of-plane bending moment, M_y
$Z_{Tip, Mx}$	Z-axis displacement of the fitting's tip (corner) due to the x-axis component of applied out-of-plane bending moment, M_x
$Z_{Tip, My}$	Z-axis displacement of the fitting's tip (corner) due to the y-axis component of applied out-of-plane bending moment, M_y
α	Angle between the out-of-plane bending moment vector and the local x-axis
α_a	Actual angle between the neutral line and the local x-axis (measured from the idealized FEM constant Z-displacement contours)
α_e	Estimated angle between the neutral line and the local x-axis ((computed using elasticity and geometry)
β	Angle between the joint diagonal and the local x-axis

2. Introduction

Validation and evaluation of the new analysis approach[1], which is a method to compute fastener tensile loads in joints loaded with out-of-plane forces and bending moments, is the subject of this article. This approach was proposed as a replacement to the superposition method[2]. The validation process entails comparing the results of this analysis approach with the results of some benchmark analysis method, namely the Finite Element Method (FEM). Experimental validation of the results of the proposed analysis approach was ruled out due to the high expenses involved.

The validation process entailed analyzing eight (8) fastener joints using the proposed analysis approach[1] and the finite element method then comparing the results of both analysis methods. Six (6) of the joints analyzed are low to medium aspect ratio joints and two (2) are high aspect ratio joints. The low to medium aspect ratio joints are: 1) 5.25"x9.75"x0.50" fitting joined with 32 fasteners; 2) 5.25"x7.25"x0.50" fitting joined with 24 fasteners; 3) 5.25"x5.25"x0.50" fitting joined with 16 fasteners, all fasteners are the same material; 4) 5.25"x5.25"x0.50" fitting joined with 16 fasteners, the two left fastener columns are steel while the two right fastener columns are titanium; 5) 9.75"x5.25"x0.50" fitting joined with 32 fasteners; and 6) 6.00"x3.50"x0.50" fitting joined with 15 fasteners. The high aspect ratio joints are: 7) 2.25"x9.75"x0.50" fitting joined with 16 fasteners; and 8) 1.00"x9.75"x0.50" fitting joined with 8 fasteners. The fitting dimensions above are Width, Height, and Thickness, respectively. The substrate/base has the same dimensions as the fitting. Both titanium and steel fasteners are 0.25" in diameter. All joints analyzed have a regular fastener pattern. Based on this pattern, the above joints are denoted 8x4, 6x4, 4x4, 4x4A, 4x8, 3x5, 8x2, and 8x1, respectively, where the first number is the number of fastener rows and the second number is the number of fastener columns. Their aspect rations are 1.857, 1.381, 1.000, 0.538, 0.583, 4.333, and 9.75, respectively. Figure 1and Figure 2 illustrate the fastener joints used in this study.

The materials selected for use in the analytical model are: 7050-T74 aluminum die forging per AMS 4107, with compressive modulus of elasticity of 10.7×10^6 psi, for the fitting, 6Al-4V titanium alloy per AMS 4965, with extensional modulus of elasticity of 16.0×10^6 psi, for the fasteners, and AISI 4130 low-alloy steel per AMS 6350, with extensional modulus of elasticity of 29.0×10^6 psi, for the steel fasteners of joint 4x4A. No material needs to be selected for the substrate/base because the analytical model assumes all extensional deformations to occur in the fasteners and all compressive deformations to occur in the fitting.

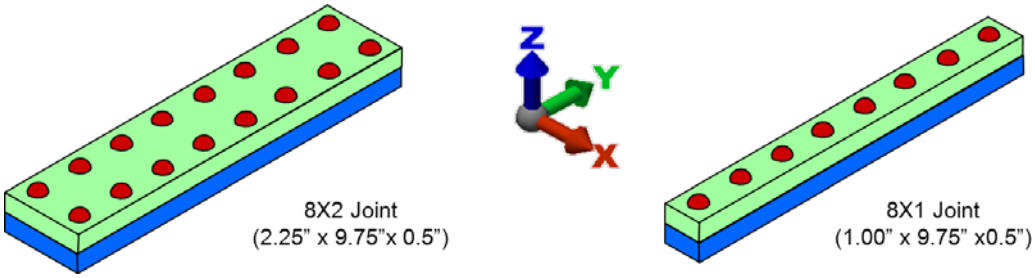

Figure 1: High Aspect Ratio Fastener Joints

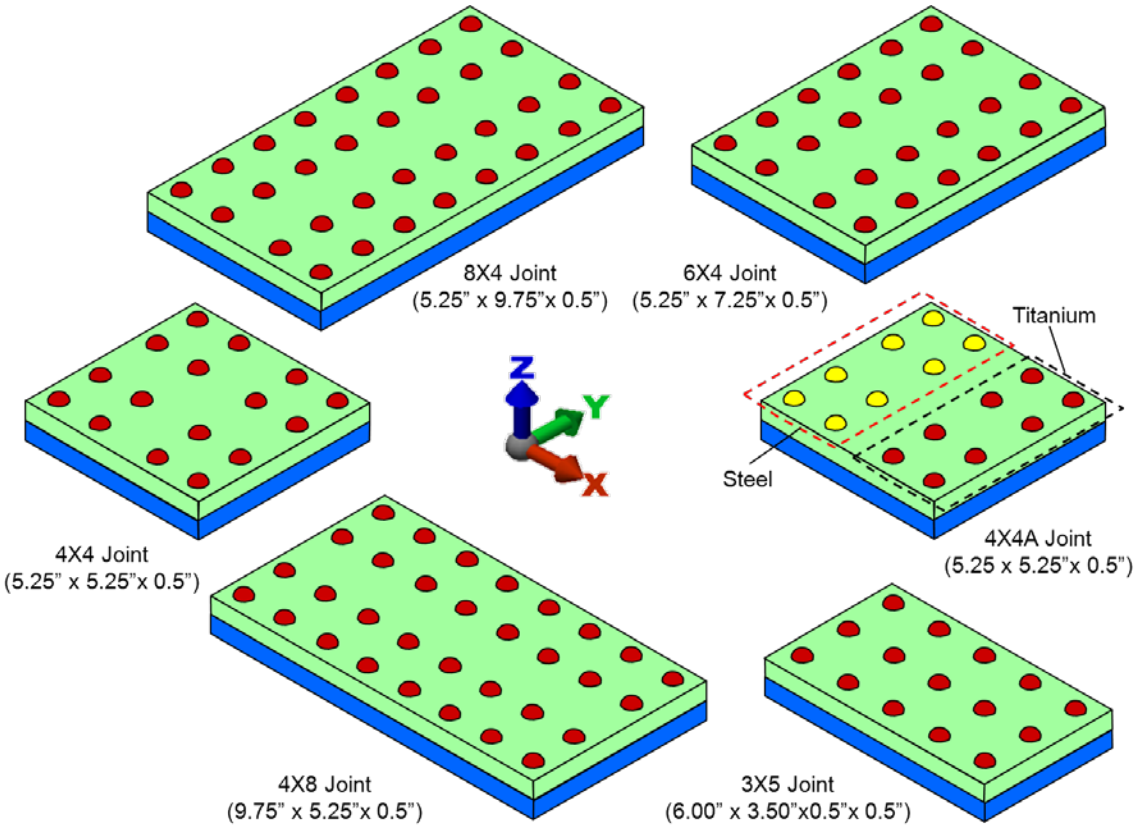

Figure 2: Low to Medium Aspect Ratio Fastener Joints

3. Finite Element Modeling

Autodesk™ Algor™ Simulation 2010 was used to construct idealized finite element models that simulate the properties and behavior of the fastener joints under investigation. All components of the fastener joints, i.e. the fitting, the substrate/base, and the fasteners, are modeled using isotropic 8-node brick elements with compatibility enforced. This means that openings, overlaps, or discontinuities are not allowed along interelement boundaries. Such compatibility can, however, overestimate the stiffness of the structure and a greater mesh density is required in the direction of the strain gradient to achieve the same level of accuracy as elements for which compatibility is not enforced. To achieve this level of accuracy, an approximate absolute mesh size of 0.065" is used for all joint components. A sample of the mesh size used is illustrated in Figure 3. The 8-node brick elements are formulated using assumed linear displacement field and 3rd order integration for moderately distorted elements.

Enforced boundary conditions are such that all six degrees of freedom are constrained at the lower surface/plane of the substrate/base while only five degrees of freedom are constrained at the lower fastener heads. Translation along the z-axis direction is unconstrained for all fasteners. Surface contact pairs are established between: 1) the upper fastener heads and the

upper surface/plane of the fitting; 2) the lower surface/plane of the fitting and the upper surface/plane of the substrate/base; and 3) the lower surface/plane of the substrate/base and the lower fastener heads. Surface contact means that the nodes on the two surfaces in the contact pair will be matched and the nodes will be free to move away from each other. If the nodes move towards each other stiffness will be applied to resist this movement. Surface contact also means that the analysis will involve an iterative process. This process is used to determine if the deflection due to the loading will cause each pair of nodes on these surface contact pairs s to be in contact or not. Figure 4 depicts the boundary conditions and surface contact pairs used in developing the idealized FEM models.

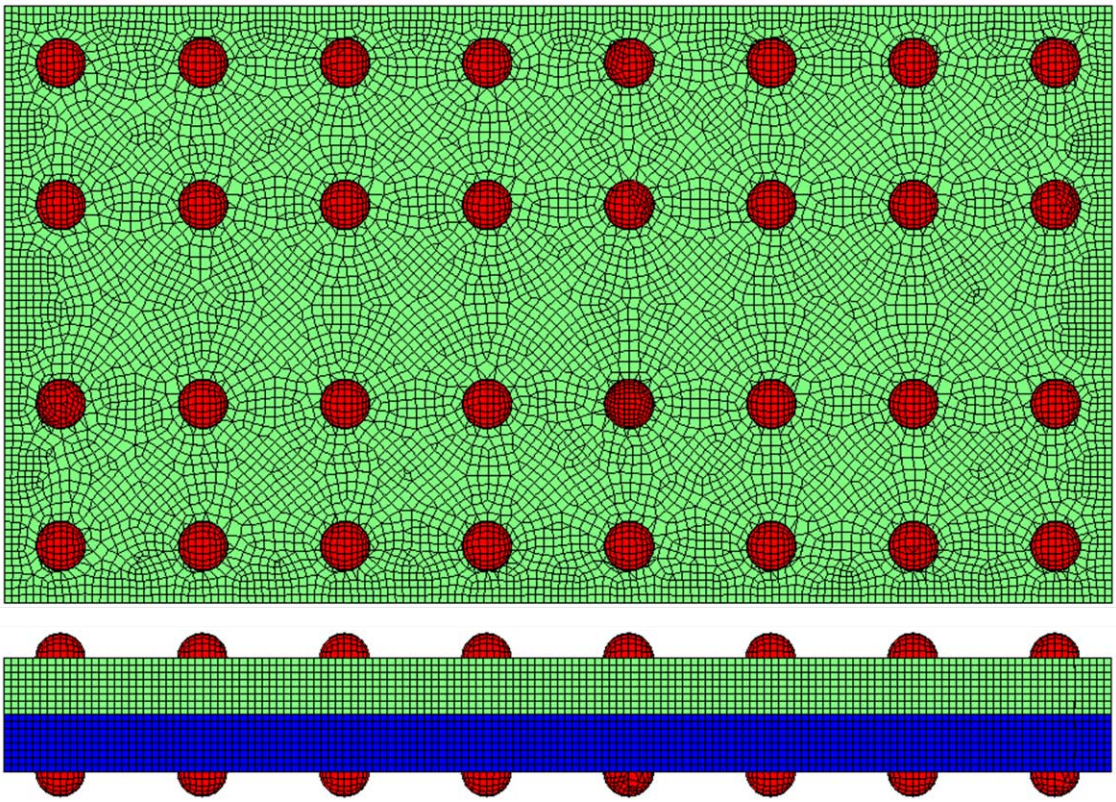

Figure 3: The Mesh Size Used For All FEM Models

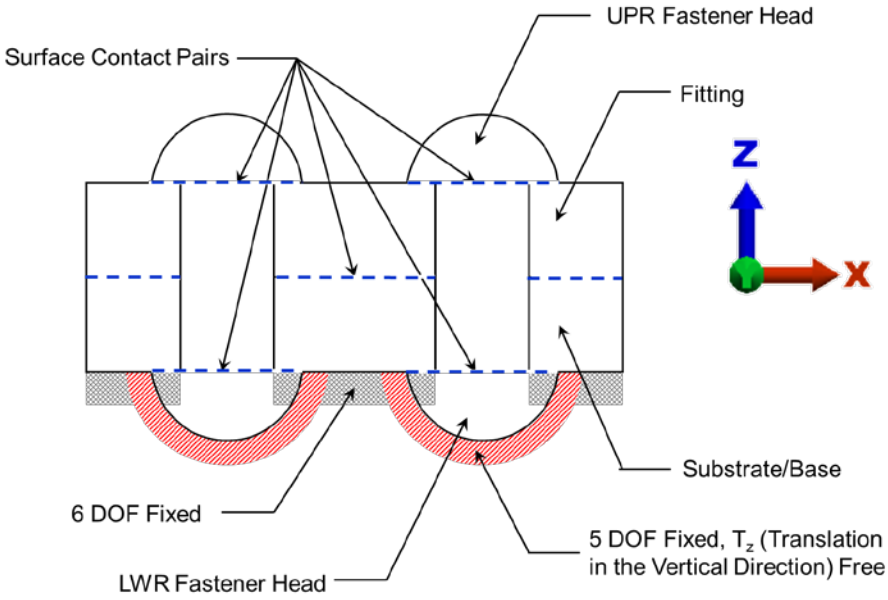

Figure 4: Boundary Conditions and Surface Contact Pairs

The AGM (arithmetic geometric mean) iterative solver[3,4,5] is used together with: 1) the **Mixed** iteration method; 2) a convergence accuracy of $1.0x10^{-6}$; and 3) 2500 maximum number of iterations. The **Mixed** iteration method simultaneously activates all inactive contact points in compression. It deactivates those nodes that are not in compression one at a time. The nonlinear structural analysis associated with the surface contact problem is linearized into many piecewise linear calculation steps. This process is continued until either equilibrium is achieved or the number of iterations exceeds the specified maximum value. Many contact problems result in unstable solutions for the first iteration. If rigid-body motion is possible, unstable solutions occur for all iterations. The reason is that the underlying mathematics results in singular or in very ill-conditioned systems when structures are not properly constrained. In order to prevent such solution problems, the **Global/Initial** stabilization method is used. This method utilizes the same small value for the stiffness throughout the model, and is only applied prior to the first iteration. It is particularly well suited for models not exhibiting rigid-body motion[6,7].

The proposed analysis approach idealizes the fitting as a plate of *infinite flexural and shear stiffness* supported by tension springs in the tension region and a compression spring in the bearing region. These springs rest on a *foundation of infinite extensional-compressive stiffness*. It also assumes that extensional deformations are allowed only in the fasteners while compressive deformations are allowed only in the bearing side of the fitting. Translating these idealizations and assumptions into the FEM models is somewhat challenging. Having infinite flexural and shear stiffness simply means that the modulus of elasticity is extremely high, which would also prevent any compressive deformation in the bearing side of the fitting. To solve this problem we revised the idealization assumptions of the FEM models to be as following:

- The joint FEM models idealize the fitting as a plate of **infinite** flexural and shear stiffness supported by tension springs in the tension region and a compression spring in the bearing region. These springs rest on a foundation of **finite** extensional-compressive stiffness.
- Extensional deformations are allowed only in the fasteners while compressive deformations are allowed only in the bearing side of the **substrate/base**.

Since the lower surface/plane of the substrate/base has all six degrees of freedom constrained, compressive deformations occur only in the bearing side of its upper surface/plane while reactions occur at the nodes of its lower surface/plane that are in contact with the lower fastener heads. A fictitious material, with modulus of elasticity of $29.0x10^{12}$ psi, is selected for the fitting. The substrate/base material is 7050-T74 aluminum die forging per AMS 4107, with compressive modulus of elasticity of $10.7x10^{6}$ psi, the fasteners are 6Al-4V titanium alloy per AMS 4965, with extensional modulus of elasticity of $16.0x10^{6}$ psi, and the steel fasteners of joint 4x4A are AISI 4130 low-alloy steel per AMS 6350, with extensional modulus of elasticity of $29.0x10^{6}$ psi.

The out-of-plane bending moment, M, is applied directly into the proposed analytical model together with the angle that its vector makes with the local x-axis, α. To apply loads to the FEM models the out-of-plane bending moment M is resolved into its local coordinate system components M_x and M_y. These bending moment components are then replaced by force couples and each force couple is applied to the corresponding opposite side surfaces/planes of the fitting. Autodesk™ Algor™ Simulation 2010 ultimately converts these force couples into distributed axial loads acting on the side surfaces/planes of the fitting and along the local z-axis as shown in Figure 5.

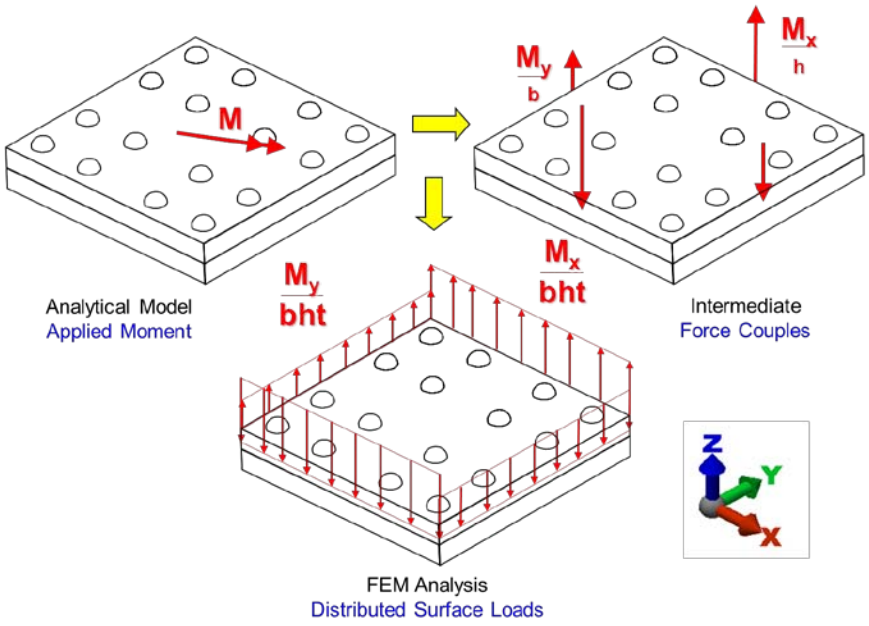

Figure 5: Loading of the Analytical and FEM Models

4. Enhancement of Proposed Analysis Approach

The original analysis approach assumed that the angle of the neutral line with respect to the local x-axis equals the angle of the out-of-plane bending moment vector with respect to same axis, as shown in Figure 7 of Reference 1. Running the cases of the first idealized FEM model, i.e. the 8x4 joint, made us realize that this assumption does not hold except when the angle of the out-of-plane bending moment vector is either 0°, 90°, or approximately (90°-β) with respect to the local x-axis. The actual angle of the neutral line is measured using the z-displacement contours of the idealized FEM model results.

The original analysis approach simply did not account for the x-y spatial distribution of extensional stiffnesses of the fasteners. To account for this effect, the original analysis approach is modified to include the following two enhancements:

- The **Equivalent Fastener**, which is a virtual fastener whose extensional stiffness equals the sum of extensional stiffnesses of all fasteners and is located at the center of gravity (centroid) of the total extensional stiffness of all fasteners. Figure 6 depicts the concept of the equivalent fastener, its location, and loading
- The **Estimated Angle of the Neutral Line** α_e. This angle depends on: the angle of the out-of-plane bending moment vector with respect to the local x-axis, α, the fitting dimensions, b and h, the extensional stiffness of the equivalent fastener, K_{EF}, and the centroid location of the total extensional stiffness of all fasteners, X_{FSCG} and Y_{FSCG}. The equations below are used in computing the estimated angle of the neutral line, α_e.

Centroid of the total extensional stiffness of all fasteners:

$$X_{FSCG} = \frac{\sum_i K_i \cdot X_i}{\sum_i K_i}$$

$$Y_{FSCG} = \frac{\sum_i K_i \cdot Y_i}{\sum_i K_i} \qquad (1)$$

Assuming any value for the out-of-plane bending moment, e.g. MVal, its components are:

$$M_x = MVal \cdot \cos(\alpha)$$
$$M_y = MVal \cdot \sin(\alpha) \qquad (2)$$

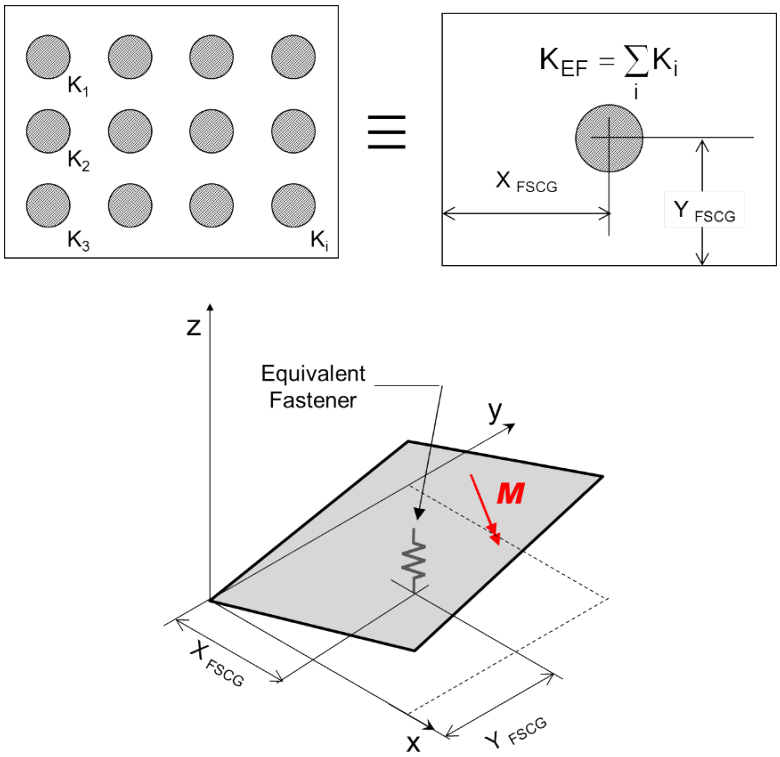

Figure 6: The Equivalent Fastener

Assuming the point of maximum bearing pressure PMBP to be at the origin of the local coordinate system as shown in Figure 7, which is the case when -90° < α < 0°, the reactions in the equivalent fastener due to the above out-of-plane bending moment components are:

$$R_{EF,\,M_x} = \frac{M_x}{Y_{FSCG}}$$
$$R_{EF,\,M_y} = \frac{M_y}{X_{FSCG}} \qquad (3)$$

Extensional deformations in the equivalent fastener due to the above out-of-plane moment components are:

$$Z_{EF,\,M_x} = \frac{R_{EF,\,M_x}}{K_{EF}} = \frac{M_x}{Y_{FSCG} \cdot \sum_i K_i}$$
$$Z_{EF,\,M_y} = \frac{R_{EF,\,M_y}}{K_{EF}} = \frac{M_y}{X_{FSCG} \cdot \sum_i K_i} \qquad (4)$$

Z-axis displacement of the fitting's tip (corner) due to the above out-of-plane bending moment components are:

$$Z_{Tip,\,M_x} = \frac{Z_{EF,\,M_x} \cdot h}{Y_{FSCG}}$$
$$Z_{Tip,\,M_y} = \frac{Z_{EF,\,M_y} \cdot b}{X_{FSCG}} \qquad (5)$$

The estimated angle of the neutral line with respect to the local x-axis depends on whether $Z_{Tip,\,M_x} > Z_{Tip,\,M_y}$ or vice versa

If $Z_{Tip,\,M_x} > Z_{Tip,\,M_y}$:

$$X_{angcorr} = b$$
$$Y_{angcorr} = h \cdot \frac{Z_{Tip,\,M_y}}{Z_{Tip,\,M_x}} \qquad (6)$$

If $Z_{Tip,\,M_x} < Z_{Tip,\,M_y}$:

$$X_{angcorr} = b \cdot \frac{Z_{Tip,\,M_x}}{Z_{Tip,\,M_y}}$$
$$Y_{angcorr} = h \qquad (7)$$

Finally

$$\alpha_e = \tan^{-1}\left(\frac{Y_{angcorr}}{X_{angcorr}}\right) \qquad (8)$$

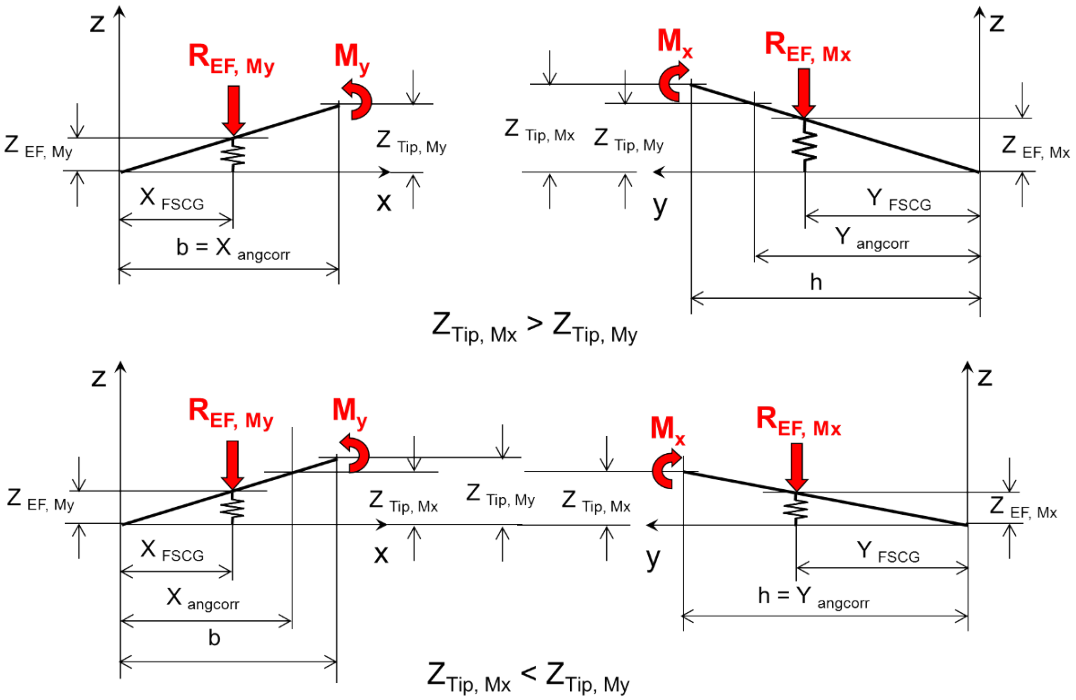

Figure 7: Determining the Estimated Angle of the Neutral Line, α_e

In the above mathematical formulation, compression in the bearing area is neglected because the number of unknowns (3) would be larger than the number of equations of equilibrium (2), i.e. ΣM=0 and ΣZ=0. This simplification made these enhancements to the original analysis approach possible. It is believed that some of the differences between the results of the enhanced analysis approach and the idealized FEM models are attributed to this simplification.

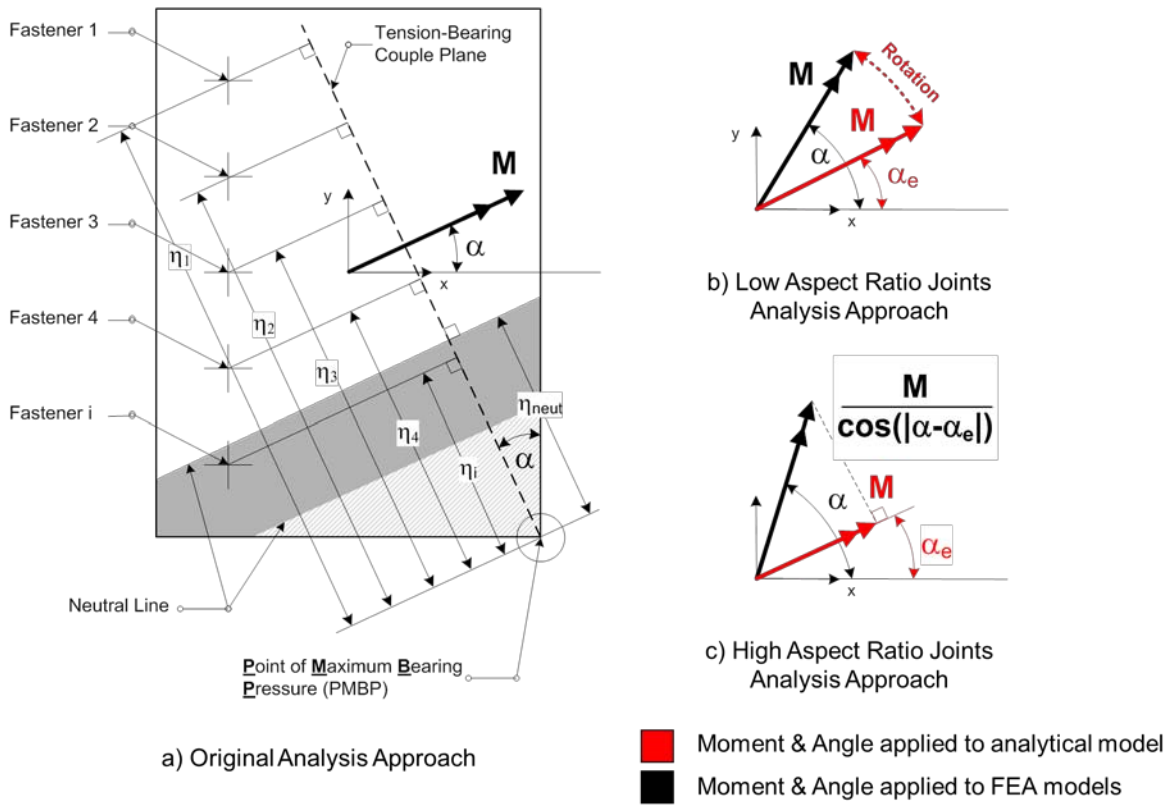

Figure 8: Original and Enhanced Analysis Approach

Figure 8a depicts the original analysis approach, which assumed that the neutral line has the same angle, with respect to the local x-axis, as the applied out-of-plane bending moment vector. The enhanced analysis approach assumes that the out-of-plane bending moment is rotated from angle α to angle α_e, as depicted in Figure 8b. This assumption does not work well for high aspect ratio joints, which demonstrated high differences between the results of the enhanced analysis approach and the idealized FEM models. A modified assumption is used for this type of fittings, which simply postulates that the projection of the applied out-of-plane bending moment vector on the direction of the estimated angle of the neutral line is used for the enhanced analysis approach. The later assumption worked well for the high aspect ratio fittings. The validation roadmap for the enhanced analysis approach is depicted in Figure 9.

5. Validation Results, Comparisons, and Discussions

The intention of this study has never been to validate the tensile load results of every individual fastener in any of the eight joints analyzed. Rather, our intention is to validate the total tensile load in all fasteners and the highest tensile load of all fastener results. The later drive the fastener design in any joint. We also needed to validate the concept of the equivalent fastener and the estimated angle of the neutral line.

The z-displacement contours of the idealized FEM models' results are illustrated in Figure 17 through Figure 24 together with the respective angle of applied out-of-plane bending moment vector, α, the estimated angle of the neutral line, α_e, and the actual angle of the neutral line, α_a. As stated before, these angles are with respect to the local x-axis. Figure 10 depicts the estimated and actual angles of the neutral line, α_e and α_a respectively, versus the angle of applied out-of-plane bending moment vector. Values of the estimated and actual angles of the neutral line coincide for 0°, 90°, and approximately (90°-β) moments for all analyzed joints. The difference at other angles of the out-of-plane bending moment vector are postulated to be due to neglecting compressive, flexural, and shear deformations when computing the estimated angle of the neutral line.

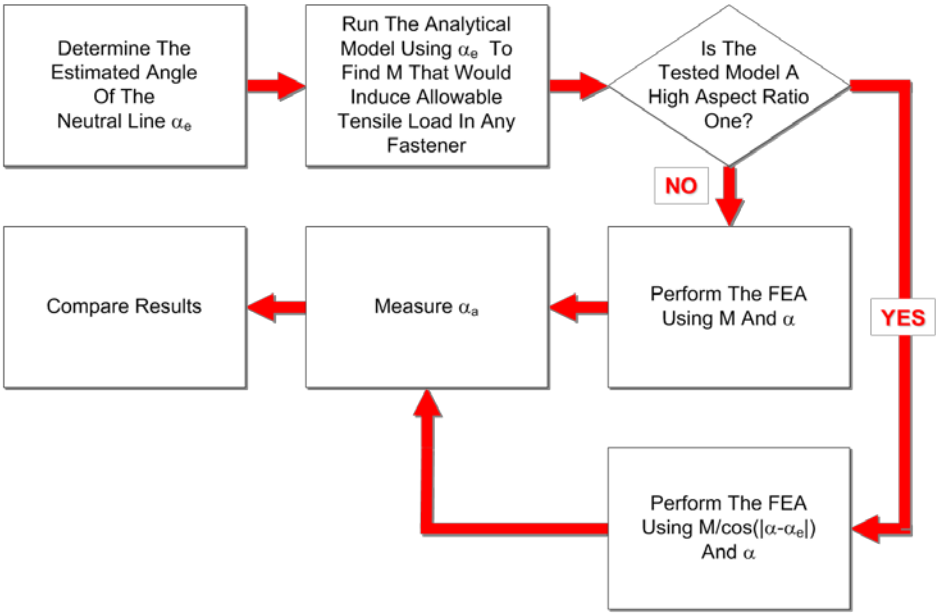

Figure 9: Validation Roadmap for Enhanced Analysis Approach

The percentage difference between the predictions of the enhanced analytical model for the low to medium aspect ratio joints and those of the idealized FEM models are depicted in Figure 11 for the total fastener loads and Figure 12 for the maximum fastener load. With the exception of only two cases, the percentage difference between the predictions of the enhanced analytical model and the idealized FEM models are within ±10%. Figure 13 depicts the percentage difference between the predictions of the enhanced analytical model for the high aspect ratio joints and those of the idealized FEM models. Similar to the low to medium aspect ratio models, the percentage difference between the predictions of the enhanced analytical model and the idealized FEM models are within ±10%. The percentage difference between predictions is defined as:

$$\%\text{Diff} = \frac{P_{MOD} - P_{FEM}}{P_{FEM}} \cdot 100 \qquad (9)$$

An added merit for using the enhanced analytical model is depicted in Figure 14. As illustrated, the processing times for the finite element models are extremely higher than the processing time for the enhanced analytical model. The processing times for the finite element models are based on using Dell Precision Mobile Workstation M6300 with Intel Core 2 Duo CPU T9300 @ 2.50 GHz and 8 GB of 2.49 GHz RAM and Autodesk Algor Simulation 2010 iterative AGM solver. The analytical model processing time is less than one (1) minute for any analyzed joint or moment angle.

6. Conclusions

The results of the idealized FEM models are in good agreement with the results of the enhanced analysis approach. Percentage differences between the results of the enhanced analysis approach and the results of the idealized FEM models are within ±10% for both the total tensile load of all fasteners and the highest fastener tensile load across all joints analyzed. Introducing the spatial distribution of the extensional stiffnesses of the fasteners as an enhancement to the analysis approach proposed in Reference 1 was pivotal for obtaining such good agreement of validation results. The difference between the results of the enhanced analysis approach and idealized FEM models is attributed to: 1) the fastener flexural and shear deformation, particularly in the direction of the shorter dimension of the fitting; and 2) the anomalies of the bearing region. These factors are depicted in Figure 15 and Figure 16. The enhanced analysis approach does not account for either of these factors.

The fact that the validation process is based on idealized FEM models, which assume no flexural or shear deformations in the fitting, does not in any way discredit the conclusions of this effort mainly because the proposed analysis approach assumes such simplifications. Our next task is to validate the results of the enhanced analysis approach presented in this article using FEM models that allow flexural and shear deformations in the fitting. The true potential of the TBC enhanced analysis approach can only be evaluated after such work is complete.

7. Acknowledgement

The authors wish to acknowledge with sincere thanks the help and cooperation of Mr. Edward Simmons and Mr. Rajesh Radhakrishnan of Autodesk Inc. Mr. Simmons helped us to acquire the Algor software package at an appealing discounted price and Mr. Radhakrishnan provided us with technical support, help, and guidance throughout the finite element analysis phase of this effort. Without their unfailing assistance and support the completion of this work was highly doubtful.

8. References

[1] Daken, Hatem H., "Tension-Bearing Couples (TBC): An Analysis Approach for Fastener Joints Loaded By Out-Of-Plane Forces and Compound Bending Moments," 13th International Conference on Aerospace Sciences & Aviation Technology, ASAT-13, May 26 – 28, 2009

[2] Bogis, Haitham A. et al, "Computer-Aided Design of Riveted and Bolted Joints Under Compound Loading," Mechanical Engineering Department, King Abdulaziz University, Jeddah, Saudi Arabia

[3] Borwein, J. M. and Borwein, P. B., "On the Mean Iteration…..," Mathematics Of Computation, Volume 53, Number 187, July 1989, Pages 311-326, http://www.jstor.org/pss/2008364

[4] "Iterative Methods," Wikipedia, http://en.wikipedia.org/wiki/Iterative_method

[5] "AGM Method," Wikipedia, http://en.wikipedia.org/wiki/AGM_method

[6] Wilson, E. A. and Parsons, B., "Finite Element Analysis Of Elastic Contact Problems Using Differential Displacements," International Journal for Numerical Methods in Engineering, Volume 2 Issue 3, Pages 387 – 395, June 2005

[7] "Autodesk™ Algor™ Simulation 2011 Help," Autodesk Center for Mechanical Simulation Technology, Finite Element Analysis, Simulation, and Design Optimization, http://download.autodesk.com/us/algor/userguides/index.html

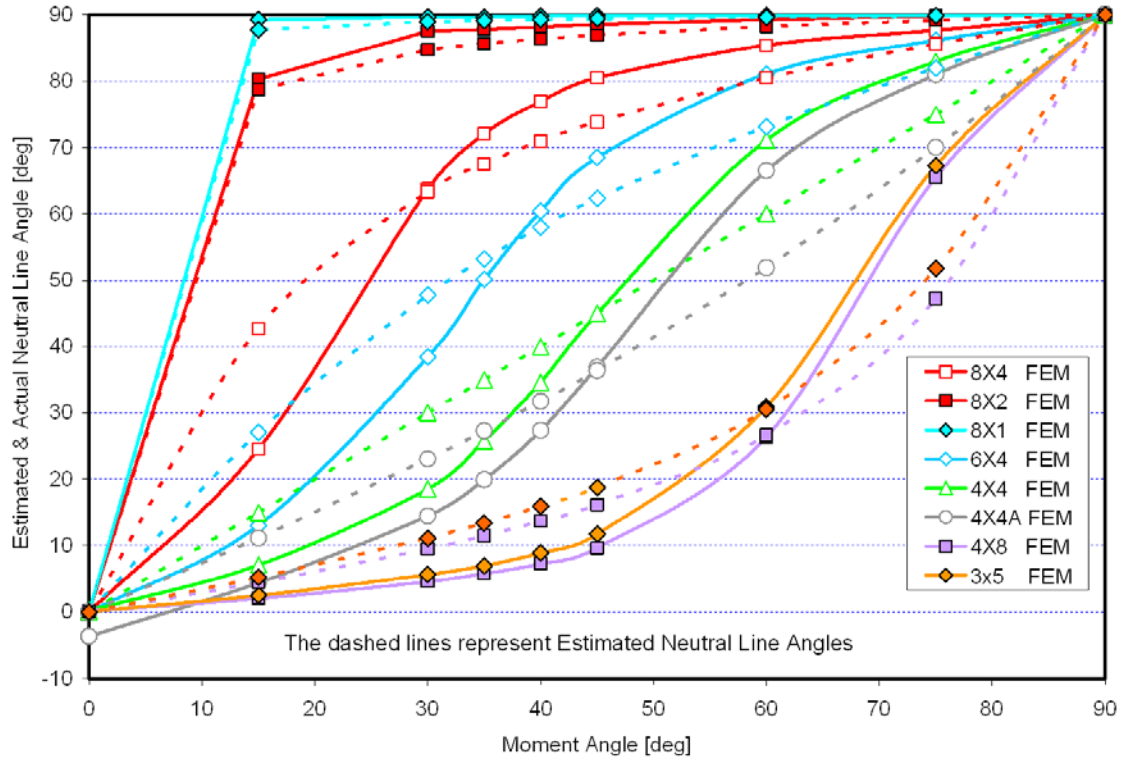

Figure 10: Estimated and Actual Neutral Line Angles Versus Applied Moment Angle

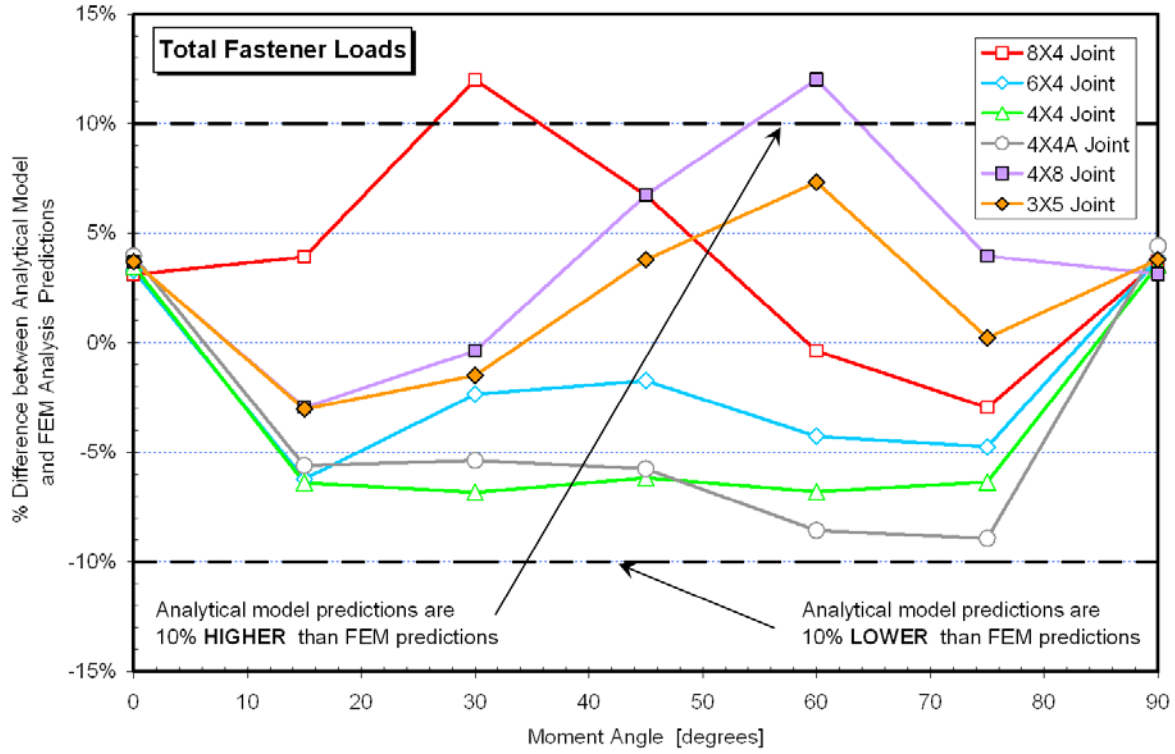

Figure 11: Percent Difference between Enhanced Analytical Model and FEM Analysis Predictions for Total Fastener Loads – Low to Medium Aspect Ratio Joints

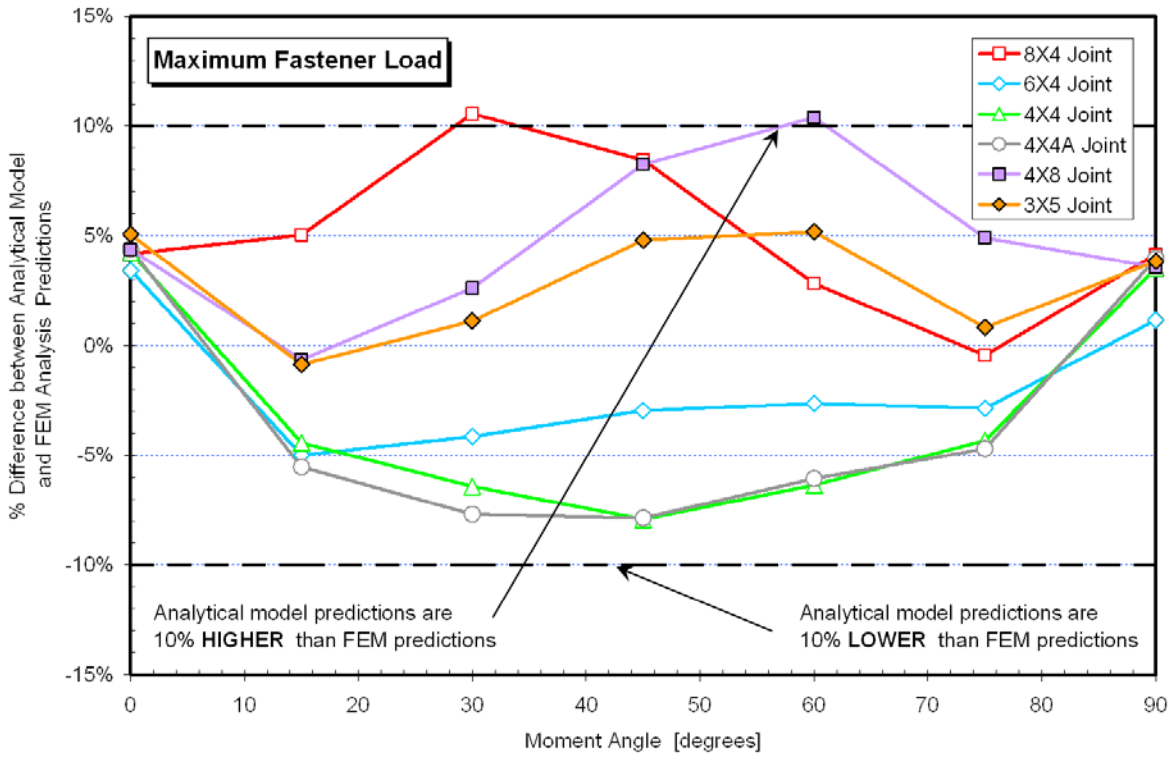

Figure 12: Percent Difference between Enhanced Analytical Model and FEM Analysis Predictions for Maximum Fastener Load – Low to Medium Aspect Ratio Joints

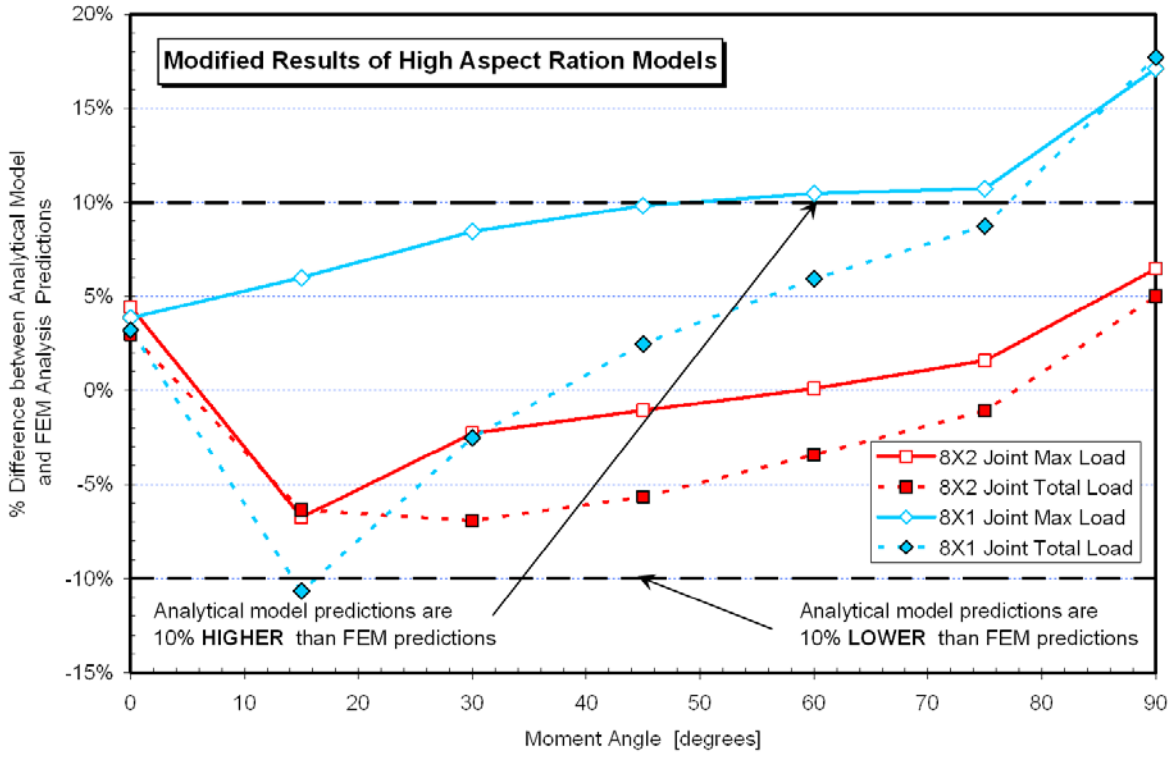

Figure 13: Percent Difference between Enhanced Analytical Model and FEM Analysis Predictions for Maximum and Total Fastener Loads – High Aspect Ratio Joints

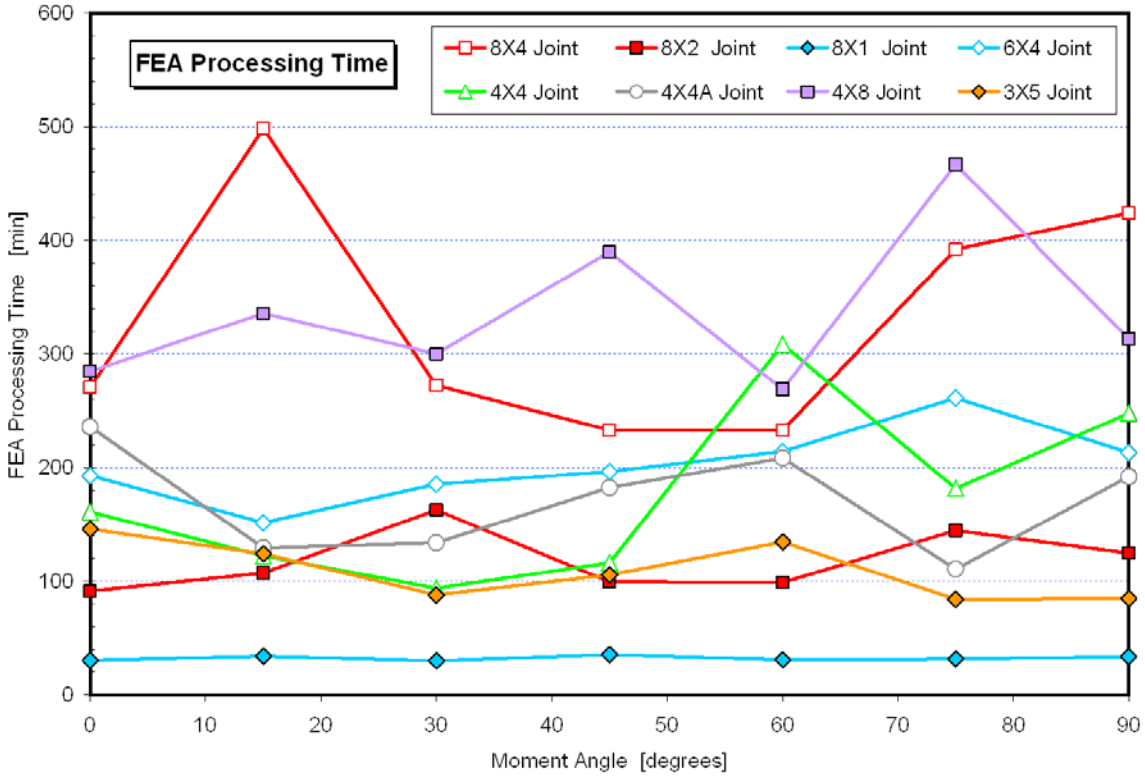

Figure 14: Processing Time for the Finite Element Analysis Models

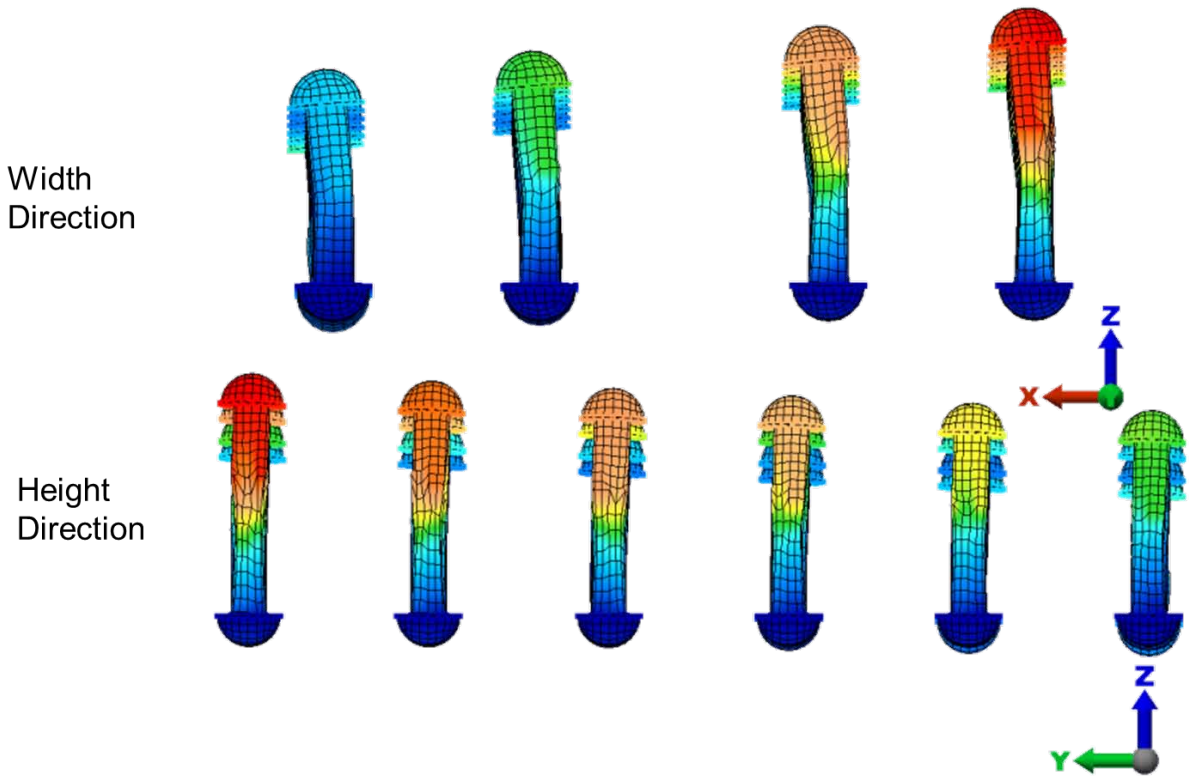

Figure 15: Fastener Flexural and Shear Deformations Along the Short (x-axis) and Long (y-axis) Dimensions of the 6x4 Fastener Joint

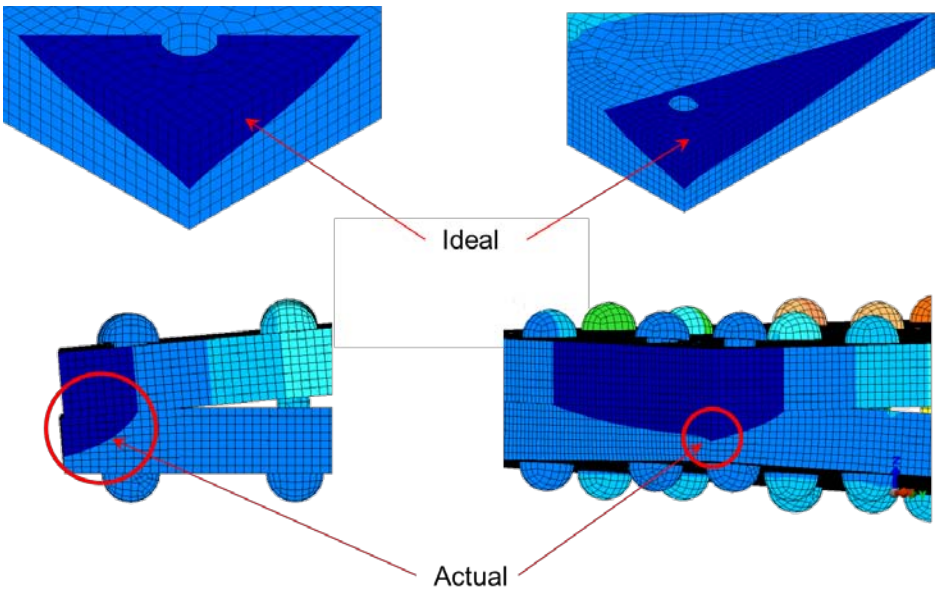

Figure 16: Bearing Area Anomalies Demonstrated by the FEM Models

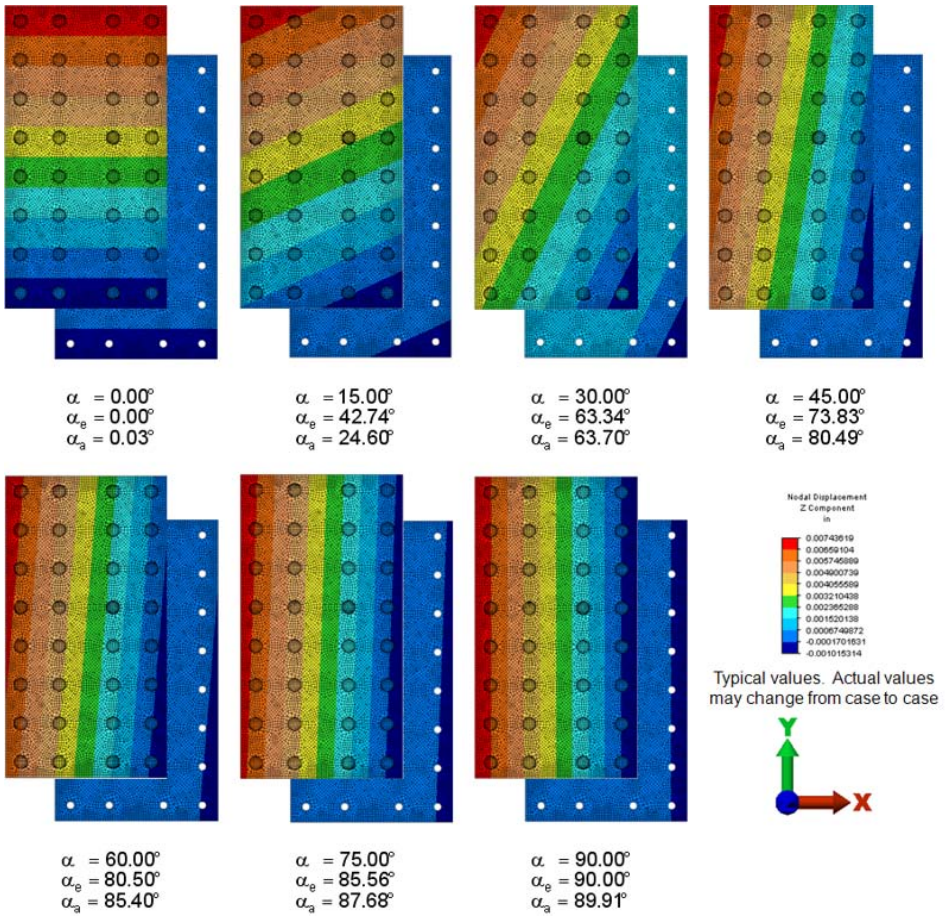

Figure 17: FEM Results Z-displacement Contours, Angle of Applied Out-Of-Plane Moment, and Actual and Estimated Angles of the Neutral Line for the 8x4 Joint

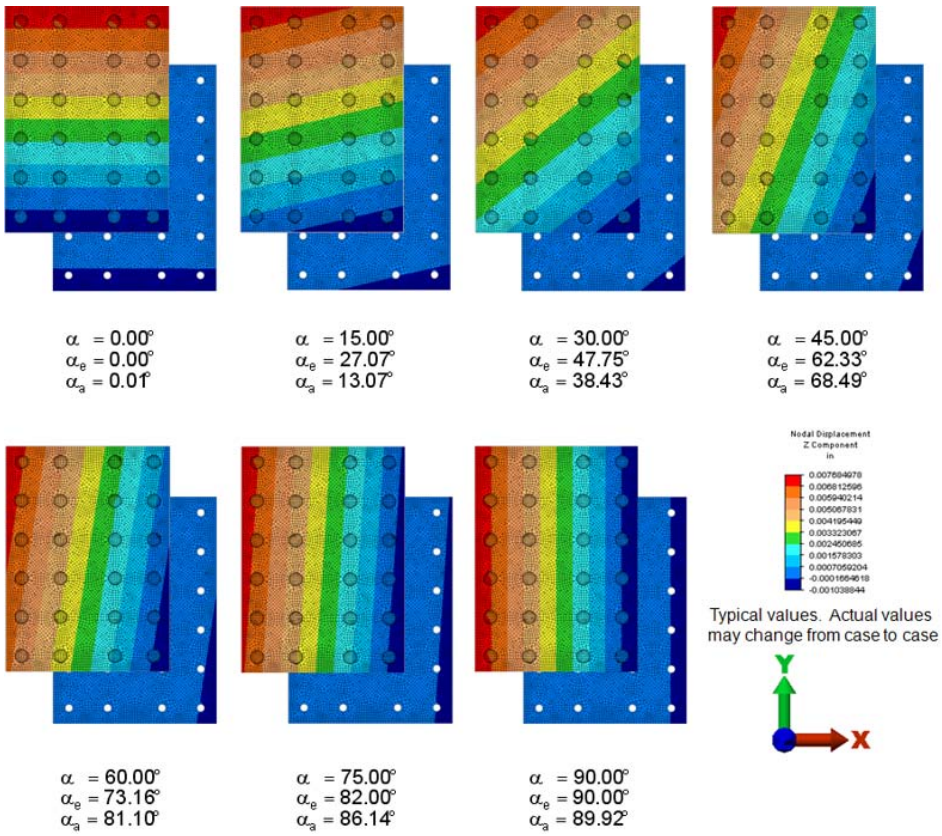

Figure 18: FEM Results Z-displacement Contours, Angle of Applied Out-Of-Plane Moment, and Actual and Estimated Angles of the Neutral Line for the 6x4 Joint

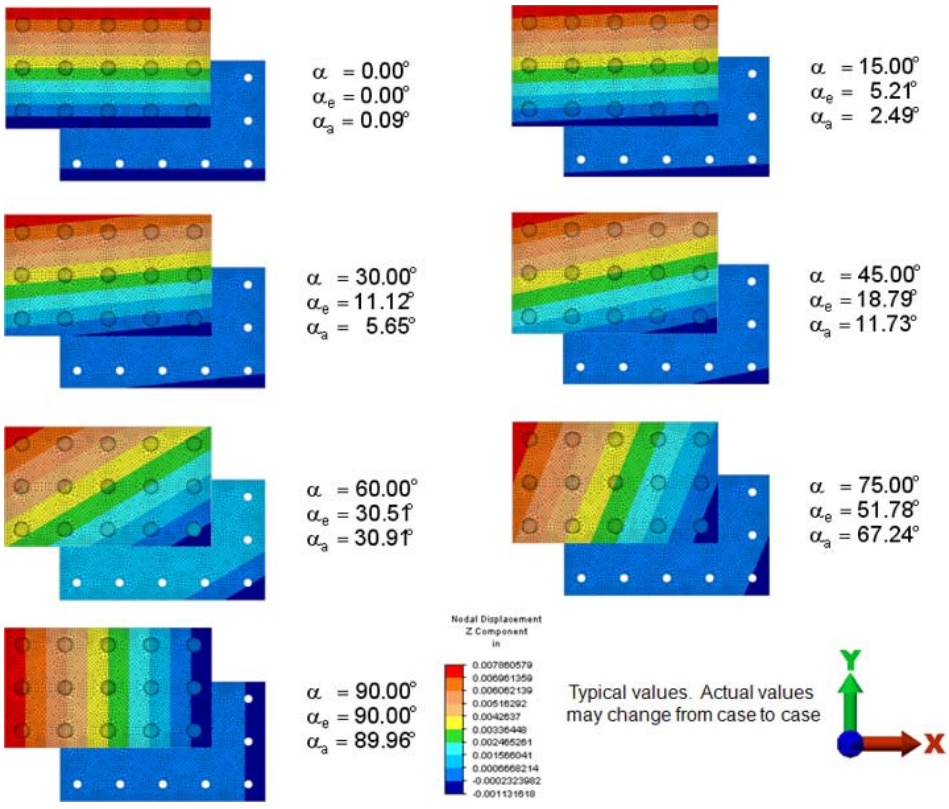

Figure 19: FEM Results Z-displacement Contours, Angle of Applied Out-Of-Plane Moment, and Actual and Estimated Angles of the Neutral Line for the 3x5 Joint

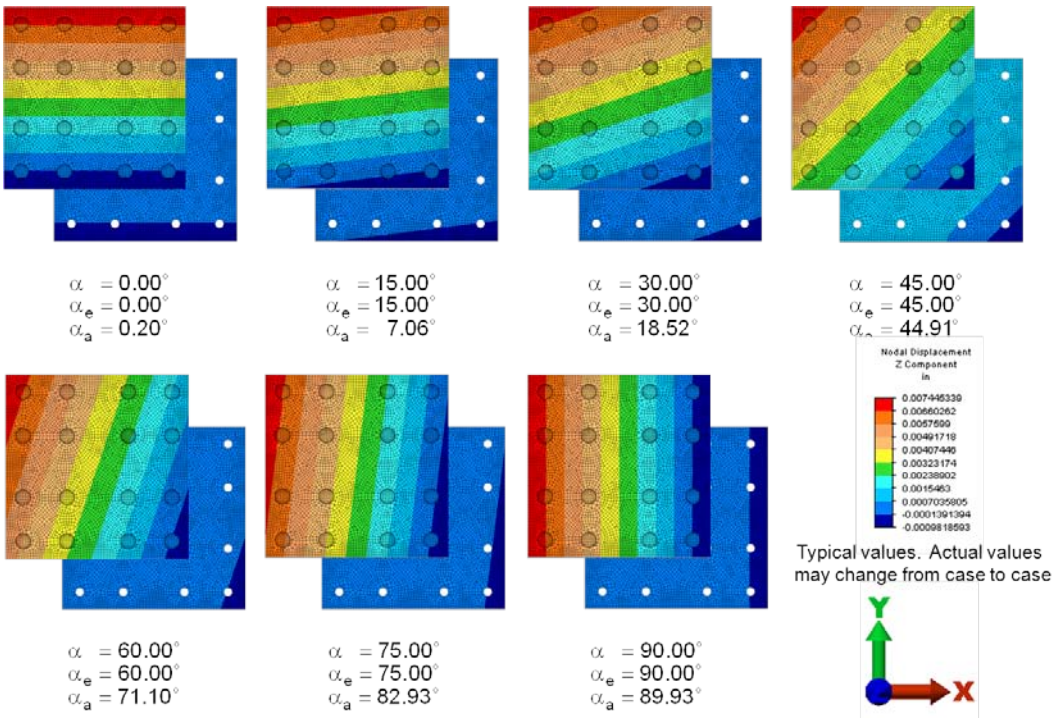

Figure 20: FEM Results Z-displacement Contours, Angle of Applied Out-Of-Plane Moment, and Actual and Estimated Angles of the Neutral Line for the 4x4 Joint

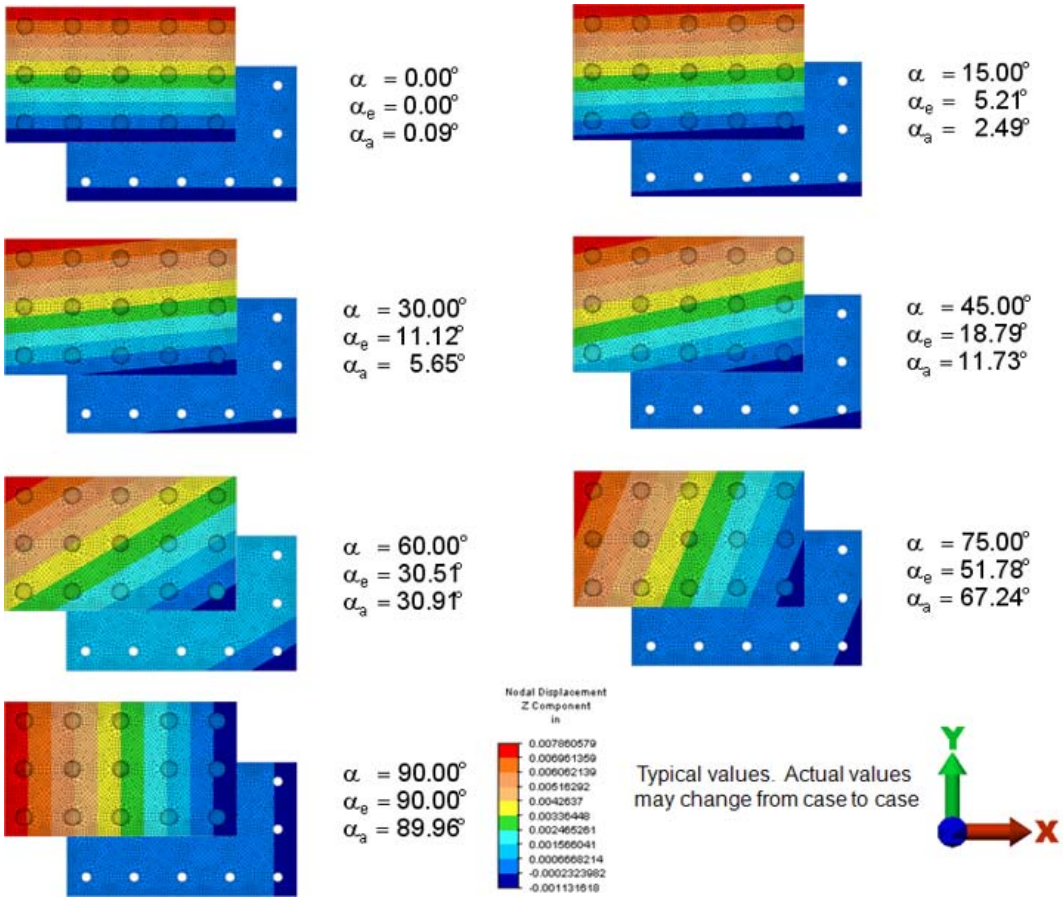

Figure 21: FEM Results Z-displacement Contours, Angle of Applied Out-Of-Plane Moment, and Actual and Estimated Angles of the Neutral Line for the 4x4A Joint

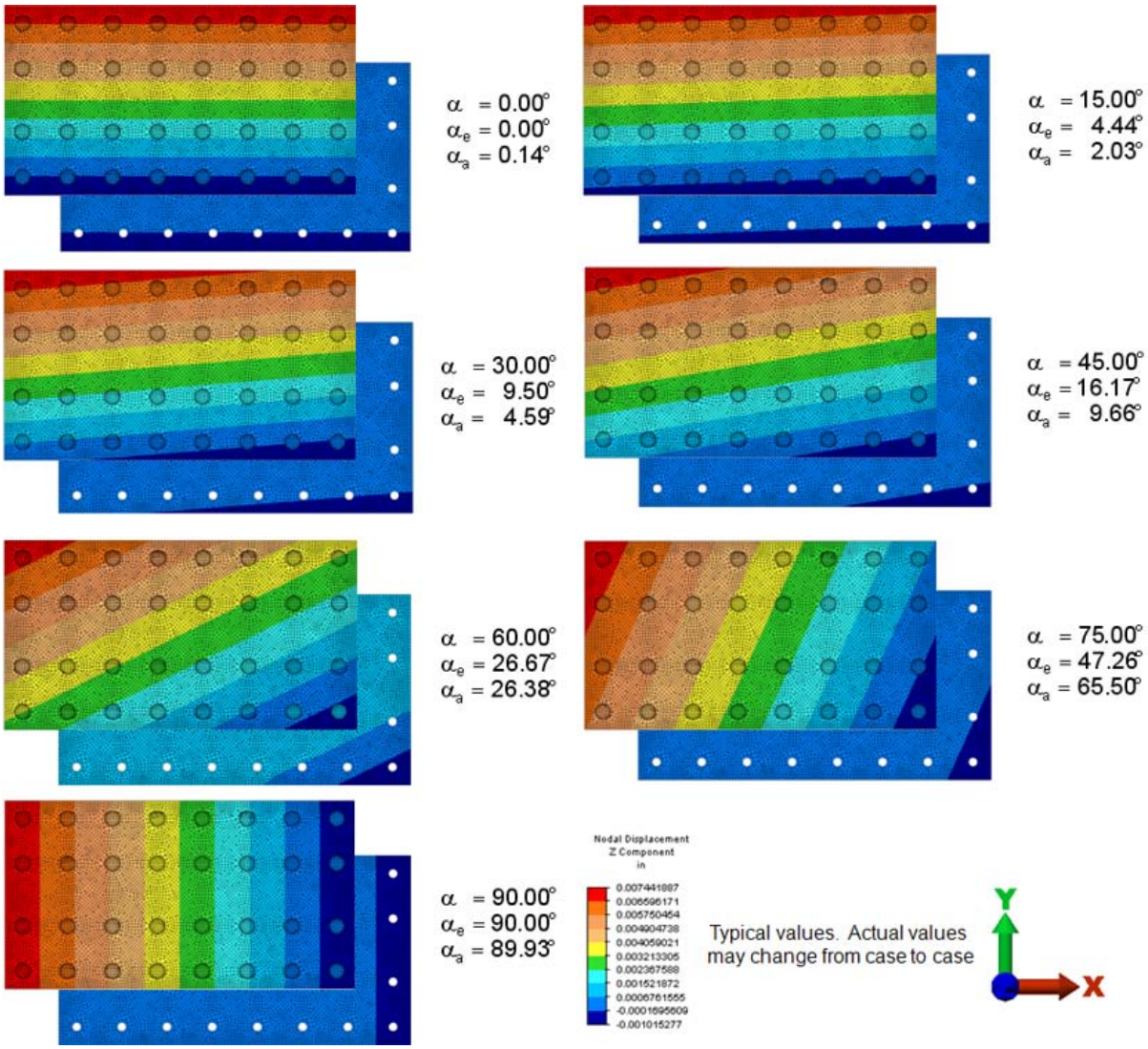

Figure 22: FEM Results Z-displacement Contours, Angle of Applied Out-Of-Plane Moment, and Actual and Estimated Angles of the Neutral Line for the 4x8 Joint

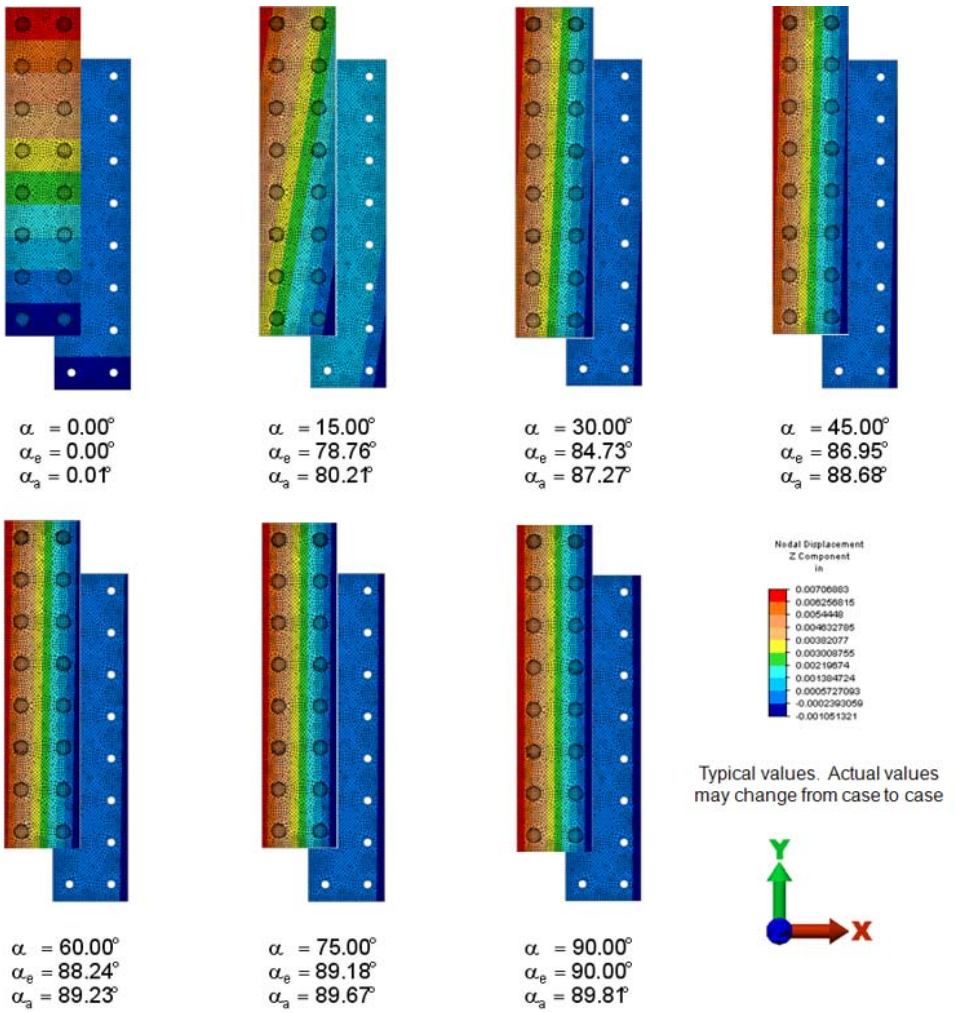

Figure 23: FEM Results Z-displacement Contours, Angle of Applied Out-Of-Plane Moment, and Actual and Estimated Angles of the Neutral Line for the 8x2 Joint

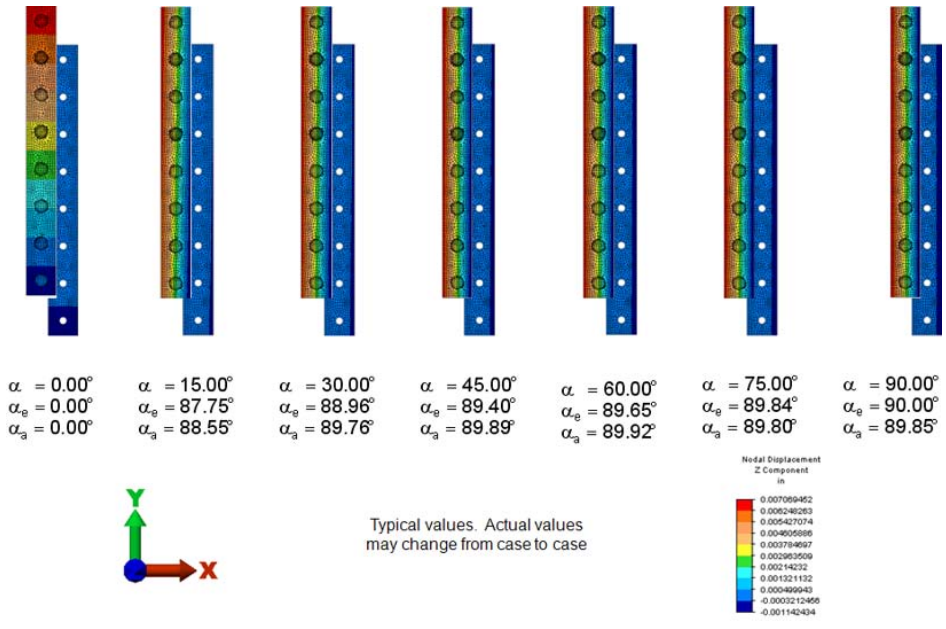

Figure 24: FEM Results Z-displacement Contours, Angle of Applied Out-Of-Plane Moment, and Actual and Estimated Angles of the Neutral Line for the 8x1 Joint